Hollow Cathode and Thruster Discharge Chamber Plasma Measurements Using High-Speed Scanning Probes

IEPC-2005-269

Presented at the 29th International Electric Propulsion Conference, Princeton University, October 31 – November 4, 2005

Kristina K. Jameson*, Dan M. Goebel†, and Ron M. Watkins‡
Jet Propulsion Laboratory, California Institute of Technology, Pasadena, CA 91109

Abstract: With the successful performance of the NSTAR ion thruster in the Deep Space 1 mission, coupled with the recently completed 30,352 hour extended life test (ELT) of the NSTAR flight spare thruster, ion thrusters have become a viable option for future NASA missions. Proposed nuclear and solar electric propulsion missions require the life of thrusters to exceed well beyond 30,000 hours, and the life of the cathode assembly and discharge are of specific concern. In an effort to understand cathode discharge plasmas, two separate cathode geometries have been investigated: a 0.635 cm-dia. NSTAR cathode and a 1.5 cm-dia. NEXIS cathode. Several probe diagnostics have been used internal and external to the hollow cathodes to measure the local plasma parameters. Axially scanning, miniature high speed pneumatic Langmuir probes have been used to investigate the plasma parameters inside the cathode insert, in the cathode orifice and in the keeper region. For both cathodes, plasma potentials are found vary with discharge parameter and to increase gradually up to cathode orifice where a potential discontinuity exists in the orifice regions. The potential then continues to increase for several centimeters downstream of the keeper to a maximum near the anode potential. Radially-scanning emissive and Langmuir probes have also been used to obtain plasma parameters in the localized region in front of the keeper, showing that the potential is depressed on axis directly in front of the keeper and increases radially and axially as it moves through the plasma ball. In this paper, detailed measurements of the plasma parameters internal and external to the cathode will be presented for the NSTAR cathode up to 13.1A of discharge current and for the NEXIS cathode up to 25A of discharge current.

Nomenclature

A	=	probe area
e	=	electron charge
I	=	probe current
k	=	Boltzman's constant
M	=	ion mass
m	=	electron mass
n	=	plasma density
T_e	=	electron temperature
α	=	Plasma ion current coefficient

* APT Staff, Advanced Propulsion Technology Group, Kristina.K.Jameson-119791@jpl.nasa.gov.
† Principal Scientist, Advanced Propulsion Technology Group, Dan.M.Goebel@jpl.nasa.gov.
‡ Member of the Engineering Staff, Advanced Propulsion Technology Group, Ron.M.Watkins@jpl.nasa.gov.

I. Introduction

Due to the successful 30,000 hour Extended Life Test (ELT)[1] of the NSTAR ion thruster at Jet Propulsion Laboratory and Deep Space 1 (DS1) successfully completing its mission with the NSTAR thruster as an integral part of the only on-board propulsion system, electric propulsion has now become a viable option for future NASA missions. During the post test analysis of the flight spare NSTAR thruster, it became apparent that erosion of the hollow cathode assembly has become a major life limiting mechanism for electric propulsion systems. However, the hollow cathodes appear to be the least well understood of all the components in the thruster. After nearly 40 years of investigation and decades of use in thrusters, there are no definitive models of the plasma density, temperature and potential distributions capable of describing different thermionic hollow cathode configurations and discharge conditions, and only limited empirical data of the geometry dependence on the life and performance. In order to understand hollow cathode discharges, we have undertaken a probe study of the cathode, keeper and cathode-plume regions. Fast axial and radial scanning probes are used to produce profiles of the plasma density, potential and temperature for different discharge currents and gas flow rates. This data aids in a basic understanding of the hollow cathode physics and will ultimately assist in determining cathode life.

Probing of thermionic hollow cathodes has been performed since they were invented by Lidsky[2] in the 1962. Familiar thermionic hollow cathode geometries were described by Rawlings[3] for mercury thrusters, Moore[4] for cesium thrusters, and Sovey[5] for noble-gas magnetic-cusp thrusters. The definitive probe study of a mercury hollow cathode was performed by Siegfried and Wilbur[6] in 1978. In this study, moveable probes were placed in different positions in the insert region and in the keeper/plasma plume region of a mercury cathode operated without an applied axial magnetic field. Moving the probes to new positions in steps produced profiles of density, potential, and temperature. Since the probes were of significant size to avoid melting and were moved into position manually and were stationary during data acquisition, the region near the cathode orifice was unreachable and the discharge was limited to currents below about 10 A. However, densities in excess of $1x10^{14}cm^{-3}$ were measured in the hollow cathode and axial profiles of these plasma parameters away from the cathode orifice for spot mode and plume modes operation were obtained. Hayakawa[7] published in 1989 probe data downstream from a hollow cathode in a 14 cm ring-cusp thruster, and found evidence of primary electrons in the distribution function. These experiments provided data within 1.6 cm of the cathode, but did not approach the keeper or cathode-orifice regions.

Recently, cathode and thruster discharge parameters have been investigated inside an NSTAR flight-like thruster discharge chamber using single and double Langmuir probes by Herman[8,9] and Sengupta.[10] Herman investigated the keeper region radially as close as 1.5 mm in front of the keeper out to 4 cm downstream using a reciprocating probe with dwell times in the plasma less then one second. Herman has also used emissive probes in the cathode plume region to find plasma potentials from 1.5 mm to 2 cm downstream of the keeper.[11] Sengupta investigated plasma parameters radially over a larger area inside the thruster, from 1.0 cm in front of the keeper to 10 cm downstream and radially across the discharge chamber, with a scanning probe that had dwell times also less than one second.[10] None of these investigations were capable of obtaining the plasma parameters inside the hollow cathode and in the orifice region of the keeper.

To diagnose the local plasma parameters inside the cathode, the cathode plume, and discharge chamber, a mock up of the NSTAR thruster discharge chamber was assembled in the JPL cathode test facility[12,13]. The experimental setup consists of cathode station, where either a 0.635 cm NSTAR cathode or a 1.5-cm NEXIS cathode is mounted, a water-cooled anode that simulates the 30-cm thruster body, and various diagnostics inserted into the plasma. Two small, minimally-perturbing Langmuir probes are driven axially in the system by high speed pneumatic plungers at speeds as high as 2 m/s. This fast scanning speed is required because these regions typically have high plasma densities, which can cause the small probes to over heat and melt. The cathode probe, constructed with a 0.5 mm dia. ceramic tube at the tip, is capable of being inserted from the upstream edge of the insert all the way though the cathode orifice entrance and into the keeper region. The peak plasma density inside the NSTAR hollow cathode is in the low 10^{15} cm^{-3} range while the NEXIS cathode is in the low 10^{14} cm^{-3} range. In the anode region exterior to the keeper, the density for both cathodes are in the 10^{11}-10^{13} cm^{-3} range, depending on the distance from the cathode exit and the discharge parameters. Axial potential profiles internal to the NSTAR cathode are found to be relatively flat over the 3-to-5 mm plasma contact length, with about a 6 V plasma potential for TH15 and a 9 V plasma potential for TH8. The plasma potential is found to decrease gradually upstream of this region. The NEXIS cathode potential profile is also relatively constant over the peak density region at 12 V for the nominal 25 A case and as much as 20 V for the 10 A case. The similarly constructed anode probe has a throw of up to 15 cm and can insert a Langmuir probe from the exit of the anode cylinder into the orifice of the keeper. The anode potentials vary from a low value on the order of 12 to 18 V in the cathode and keeper orifice region, which increase to a higher potential on the order

of the discharge voltage 2–to–5 cm downstream for both cathodes. Radially in the cathode plume, the density decreases when moving off axis while the potential increases to several volts above the discharge voltage 1 to 2 cm off axis. The different NSTAR and NEXIS operation levels impact both the cathode and anode potential profiles; however the electron temperature is not very sensitive to the operating condition. The temperature is less than 2 eV internal to the NSTAR cathode and 2-3 eV internal to the NEXIS cathode. The electron temperature typically is found to increase from 2-3 eV in the keeper orifice to 4-5 eV downstream for both cathodes. In this paper, detailed measurements of the plasma parameters will be presented inside the cathode and in the keeper and discharge chamber regions for the NSTAR cathode at TH8 and TH15 throttle levels and the NEXIS cathode at 10 A and 25 A operation conditions.

II. Experimental Hardware

A schematic diagram of the hollow cathode, anode, axial probe assemblies, and the radial probe is shown in Fig. 1. Two different hollow cathodes are used in these experiments: a conventional NSTAR cathode and a NEXIS cathode. The conventional NSTAR cathode[1] is constructed with a 6.35-mm diameter molybdenum-rhenium tube with a thoriated tungsten plate welded to the downstream end. This plate has a small orifice, of order 1.0 mm diameter, located on the centerline of the cathode. The NEXIS cathode has a configuration of a 1.5 cm diameter molybdenum tube with a tungsten orifice plate e-beam welded on the end, with an orifice size on the order 2-3 mm.[12] A porous tungsten insert impregnated with a low-work-function barium-calcium-aluminate mixture is placed inside both the NSTAR and NEXIS cathodes.[12,14] Electrons are emitted from this insert by field-enhanced thermionic emission ionize the neutral xenon gas inside the cathode. Electrons from this plasma are extracted at the downstream boundary and travel through the cathode orifice before entering the main discharge. The cathodes are heated by a standard co-axial sheathed heater, which is turned off during discharge operation. A graphite keeper electrode fully encloses both of the cathodes, and the keeper orifice is about 4.6 times the diameter of the cathode orifice for NSTAR and about 1.7 times the cathode orifice for NEXIS. The cathode and scanning probe system are mounted on an 8" Conflat flange installed in one port of 0.75-m diameter, 2-m long vacuum chamber. The chamber is pumped by two 10" CTI cryopumps with a combined xenon pumping speed of 1275 l/sec for xenon. The base pressure of the chamber is in the $1x10^{-8}$ Torr range, and during normal operation at less than 10 sccm of xenon flow the chamber pressure remains in the 10^{-5} Torr range.

The cathode scanning probe assembly is shown in Fig. 2, and a photograph of this assembly inside the vacuum chamber is shown in Fig. 3a. The bellows isolated pneumatic plunger for the cathode probe (not shown) is mounted exterior to the vacuum chamber on a mini-conflat flange adapter. The pneumatic drive shaft is coupled inside the

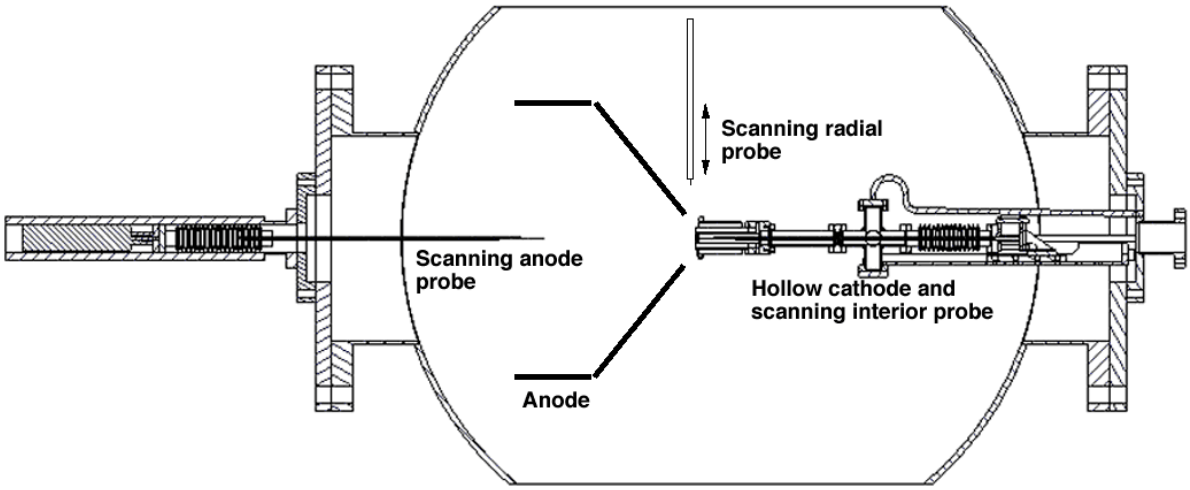

Figure 1. Schematic drawing of the cathode and anode placement along with the pneumatic scanning probes relative to the vacuum chamber.

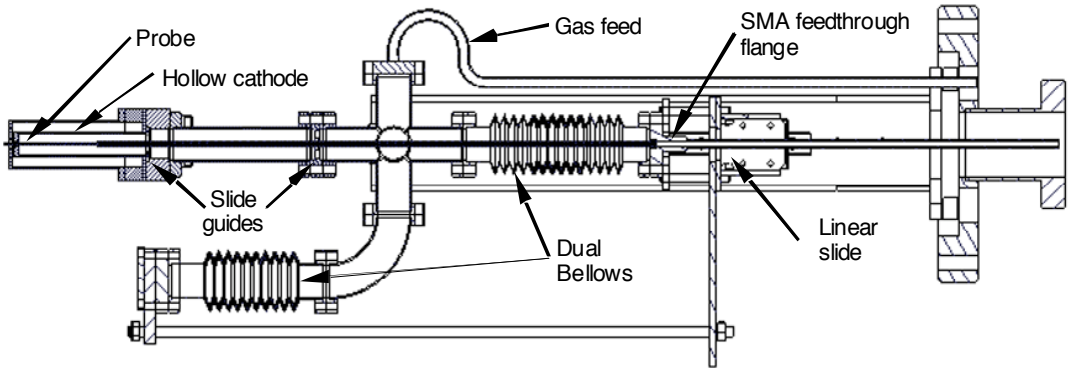

Figure 2. Schematic drawing of the pneumatic scanning probe and dual bellows arrangement used to measure the plasma parameters and pressure in the hollow cathode.

vacuum chamber to a bellows mounted between an SMA feedthrough flange connected to the probe and a six-way mini-conflat cross. Actuation of the plunger moves the SMA flange on a linear slide, compresses the bellows and inserts the single Langmuir probe into the hollow cathode. The xenon gas is controlled and measured by a digital MKS mass flow controller and injected into the hollow cathode through one port on the six-way cross. Since the plunger action will change the pressure inside the hollow cathode by decreasing the volume of the enclosed system, a second bellows on another linear slide arrangement is mounted on one of the six-way-cross ports. This second bellows is coupled to the first such that compression of the primary bellow causes a proportional expansion of the second bellows to maintain a constant volume in the system so that the pressure in the hollow cathode region is not changed during the fast probe insertion. A third port on the six-way cross is connected to a precision Baratron capacitive manometer to measure the pressure in the hollow cathode during operation.

A photograph of the cathode probe tip extending through the NEXIS cathode orifice is shown in Fig. 3b. The probe tip is 0.5 mm diameter alumina tubing with a 0.127 mm diameter tungsten wire electrode that protrudes from the small-bore ceramic tubing a distance of 0.25 mm. Even though the wire electrode is keep at a minimal length for electron collection, the probe has collected up to 5 A of current in the high density region near the orifice of the NSTAR cathode. The cathode probe is aligned axially in the system by two slide-guides internal to the cathode system. The cathode probe has a linear throw of 4 cm and can traverse the cathode at over one meter per second with a resolution of 0.25 mm. The probe tip occupies about 25% of the NSTAR cathode orifice cross sectional area, and significantly perturbs the plasma discharge if the probe is pushed too far past the upstream orifice entrance. For this reason, data is only taken prior to the probe entering the cathode orifice. Since the NEXIS cathode has a significantly larger cathode orifice, the probe tip occupies less than 3.5% of the orifice area and does not significantly perturb the plasma discharge. Therefore, information can be obtained from the probe inside the cathode orifice and in the region between the cathode and the keeper. Also shown in Fig. 3a is a solenoid coil wound on a water cooled cylinder directly around the cathode to provide an axial magnetic field of adjustable amplitude at the

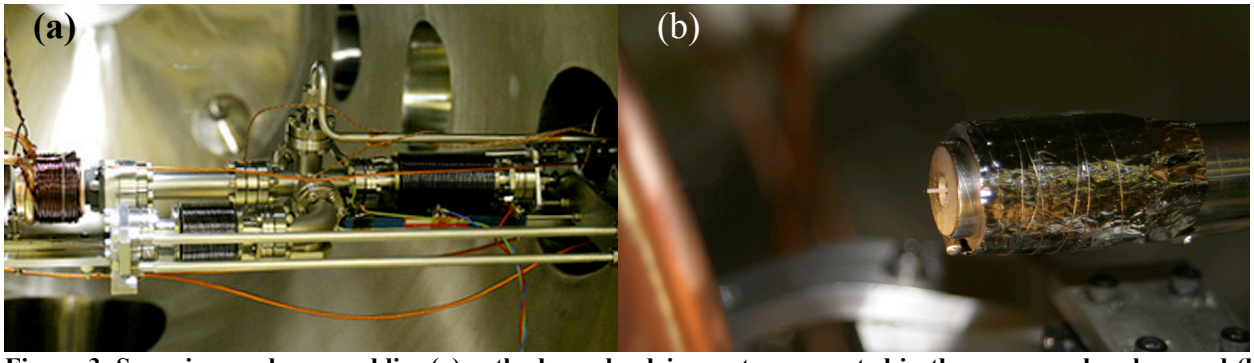

Figure 3. Scanning probe assemblies (a) cathode probe drive system mounted in the vacuum chamber, and (b) the cathode probe tip shown sticking out of the NEXIS orifice.

cathode exit that simulates the cathode field in ring-cusp thrusters. A full description of the cathode probe assembly is presented in reference 12.

The anode scanning-probe assembly is shown in Fig. 4a, where the pneumatic plunger and vacuum bellows arrangement mounted on the outside of the vacuum system are seen. The diameter of the ceramic tubing interior to the vacuum system is stepped down from 3 mm to 0.5 mm diameter in the last 3-cm section that is inserted deepest into the plasma in order to minimize perturbation to the plasma in the anode region. The exposed electrode is again a 0.127 mm tungsten wire, but has a length of typically 1.0 mm to collect sufficient current away from the keeper region to accurately determine the plasma parameters. The anode probe has nearly three times the throw of the cathode probe and 5 times the unsupported length so as to not perturb the anode-plasma, and usually moves at one meter a second with a position resolution of 0.5 mm. Very careful iterative alignment techniques are used to ensure that the anode probe is aligned with the cathode orifice and within 0.5 mm of the centerline. The anode probe can be fully inserted into the keeper orifice, although whip of the long ceramic sometimes causes the tip to touch the keeper or cathode during retraction. The anode probe inserting through the entrance of the anode and into the keeper region of a NSTAR cathode can be seen in Fig. 4b.

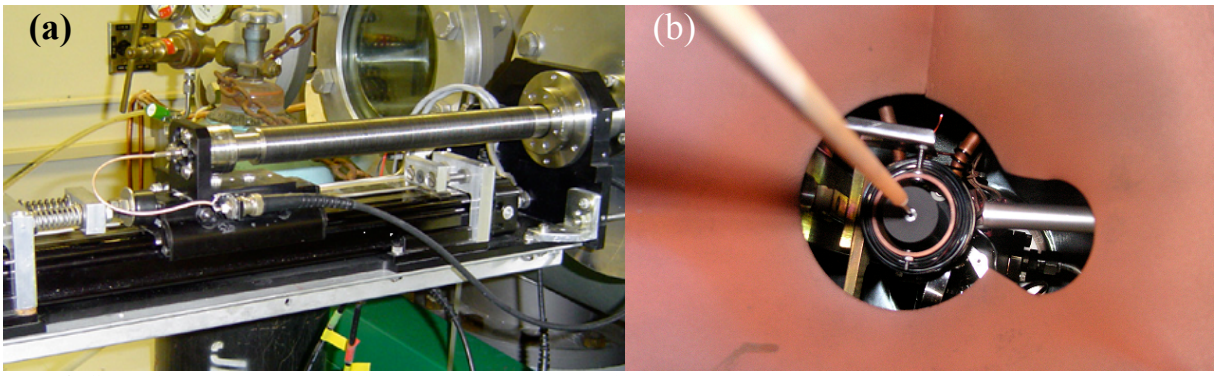

Figure 4. Scanning probe assemblies (a) anode probe drive system mounted external to the vacuum chamber, and (b) the anode probe shown entering into the NSTAR keeper region.

A radially scanning probe is also schematically shown in Fig. 1. This probe can be configured either as an emissive probe or as a Langmuir probe. It uses a pneumatic plunger external to the vacuum system, identical to the cathode-probe plunger, and is mounted to a Huntington X-Y manipulator outside the vacuum system to provide positioning relative to the keeper exit point. The radial probe has a linear throw of 4 cm, also at about one meter per second, and is aligned by a slide-guide internal to the vacuum system to obtain a position resolution of 0.25 mm. The probe can be positioned in front of the keeper as close as 1.0 mm out to 2.5 cm downstream. The emissive probe tip is a 0.127-mm diameter tungsten hairpin wire fed through two side-by-side 0.5 mm diameter alumina tubes. A floating 5 amp power supply provides the current to heat the tungsten wire electrode to emit electrons. The Langmuir probe tip is a 0.127 mm diameter tungsten wire occupying only one 0.5 mm diameter alumina tube with a probe tip length of 1.0 mm. The probe tip length is set to collect sufficient current in the lower density region downstream of the cathode, but is still relatively short as to not over heat and melt the probe tip in the high density region directly in front of the cathode orifice. When the radial probe is not in use, it is retracted into a 6.5 mm tube that is sufficiently out of the discharge plume to protect it from ion bombardment.

In order to take Langmuir traces, a bias voltage is applied to the probe tips, which is generated by a programmable waveform synthesizer that drives a Kepco bipolar power supply. The voltage waveform is a sawtooth ramp that scans from –10 to + 50 V in the anode region and from -10 to +30 in the cathode region in a time of 1 msec. In the NSTAR cathode, the cathode probe voltage is swept once per insertion to avoid overheating the probe tip in the high-density plasma near the hollow cathode orifice. A delay generator is used to take consecutive traces allowing the cathode plasma parameters to be mapped. In the NEXIS cathode, a series of voltage ramps are utilized to map the plasma parameters in a single insertion. Electron temperatures and plasma potentials are determined in less than half of the total 1 msec trace therefore the position uncertainty for the plasma parameters is on the order of 0.5 mm over most of the scan and less than 0.25 mm near the full insertion point. The probe position, voltage and current data is collected on a PC at a sample rate of 300 kHz, resulting in 300 data points in each probe characteristic curve. The plasma potential and electron temperatures are found by classical Langmuir probe analysis. The electron temperature is found by fitting an exponential curve to the electron retardation region

of the Langmuir trace. The electron temperatures have error bars about 0.5 V and the plasma potentials have error bars of ±1 V in the cathode region and up to ± 2V in the anode region.

The experimental arrangement accommodated three different anode geometries, with all anode geometries made out of cooper and water-cooled. The first geometry, being the simplest, was a cylindrical anode 5 cm in diameter and about 12 cm long. Experiments with the cylindrical anode demonstrated stable discharge for the NEXIS cathode at currents of 5 to 35 A were possible at corresponding cathode flow rates in the range of 3 to 8 sccm. At the nominal discharge current from the current-controlled power supply of 25 A and the nominal flow rates from the regulated gas system of 5.5 sccm, the discharge voltage was found to be only about 16 V. Since typical thrusters operate in the neighborhood of 25 V, it was decided to modify the anode geometry to the second geometry, a conical shape similar to the rear of NSTAR-type thrusters to raise the discharge voltage. Fig. 5a shows a picture of the cylindrical anode while Fig. 5b shows a picture of the segmented conical anode. The segmented conical anode was constructed of six isolated segments so that the current distribution could be measured as a function of the total discharge current, flow rate and magnetic field strength. This arrangement can produce discharges at 10 A at 27.3 V and at 25 A at 26.5 V. In order to accommodate the NSTAR cathode with a more representative three ring cusp magnetic field for a stable discharge, a third anode geometry was constructed, which can be seen in Fig. 5c. The third geometry has a conical section with a minimum diameter of approximately 5 cm, and is joined to the 30-cm-diameter straight cylindrical section. Also there is an adjustable gap of typically about 2 cm between the anode and keeper, thus allowing for visualization of the cathode plume and to acquire radial emissive and Langmuir probe traces. There is a solenoid coil positioned around the cathode to produce an axial magnetic field, along with two rings of permanent magnets around the anode body to simulate the NSTAR magnetic field geometry following the north-south-north structure. This anode geometry is capable of reproducing the full NSTAR Throttle Table with an emphases placed on TH8 and TH15. This arrangement can produce discharges at 8.2 A at 26.3 V representing TH8 and 13.1 A at 25.6 V representing TH15.

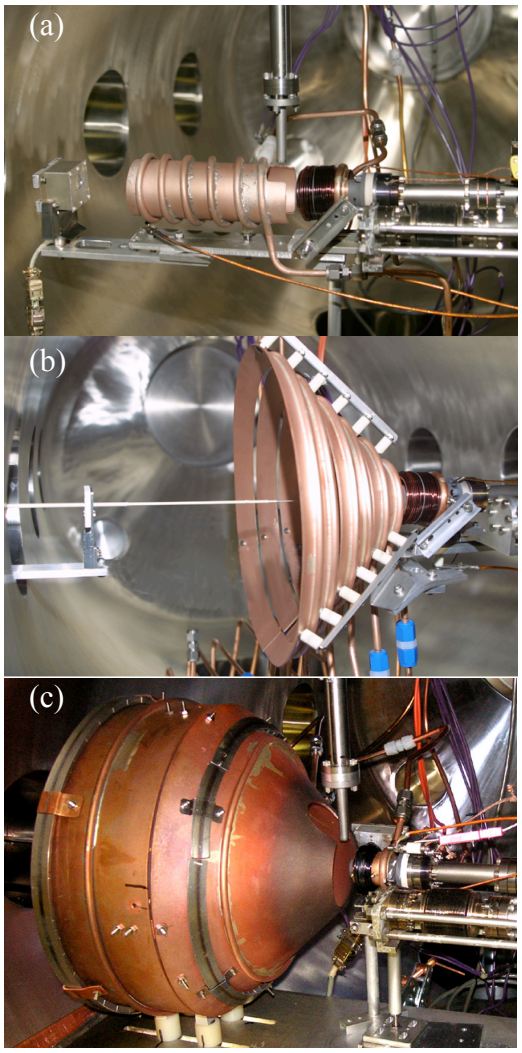

Figure 5. Water-cooled anode geometries (a) cylindrical anode (b) segmented conical anode and (c) NSTAR-like conical-cylindrical anode.

III. Experimental Results

The pressure inside the hollow cathode is measured by a Baratron manometer and recorded for different operating conditions. Internal cathode pressure for the NSTAR throttle levels is shown in Fig. 6. The neutral pressure inside the hollow cathode is relatively high for the NSTAR cathode, starting from about 4 Torr at TH4 and increasing to over 8 Torr for TH15. Even at TH4 the neutral pressure is sufficiently high to cause the plasma inside the cathode to be dominated by collisions. The flow rate is constant for TH4 and TH8, so the increase in pressure observed is due to the higher discharge current at TH08 which is heating the gas. As the flow rate and discharge current are increased from TH8 through TH15, the pressure increases significantly causing the plasma inside the cathode to become even more collisional as the throttle level is increased. The internal pressure for the NEXIS hollow cathode is shown in Fig. 7, where Fig. 7a shows the internal pressure for constant flow rate at 5.5 sccm and Fig. 7b shows the internal pressure versus flow for constant discharge current at 22 A. The NEXIS cathode shows the same trend as the NSTAR cathode; when the discharge current is increased the gas is being heated and causes the internal pressure to increase almost linearly, from 1.3 Torr at 8 A to 1.7 Torr at 26 A. Keeping the

discharge current constant and increasing the flow rate shows a more significant pressure increase, from 1.25 Torr at 4 sccm to 2.75 at 10 sccm. As flow rate is increased, the gas internal to the cathode becomes more collisional due to a higher internal pressure. Due to its larger orifice size, the pressure inside the NEXIS cathode is always noticeably lower compared to the NSTAR cathode. For example, the pressure inside the NSTAR cathode is 4 Torr at the lowest throttle level tests of about 4 A and 2.5 sccm, and internal pressures in excess of 8 Torr are observed at the highest throttle level. Therefore, the NSTAR cathode is always very collisional over its entire operating range. In contrast, the pressure inside the NEXIS cathode is less than 2.8 Torr at 22 A and 10 sccm. At the nominal operation point, which is 25 A at 5.5 sccm, the pressure inside the NEXIS cathode is only about 1.4 Torr.

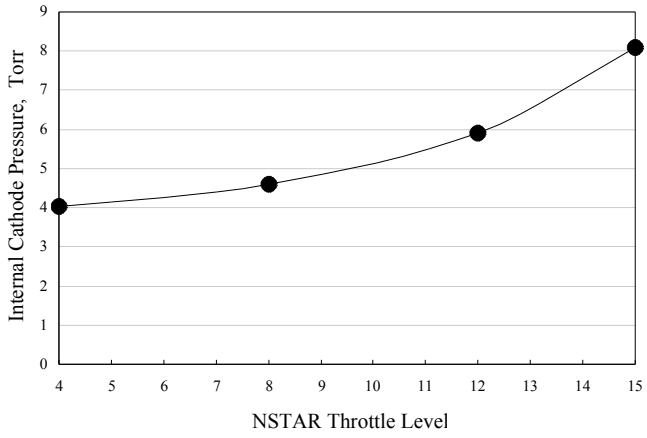

Figure 6. Pressure measured inside the 1/4" hollow cathode for various NSTAR throttle levels.

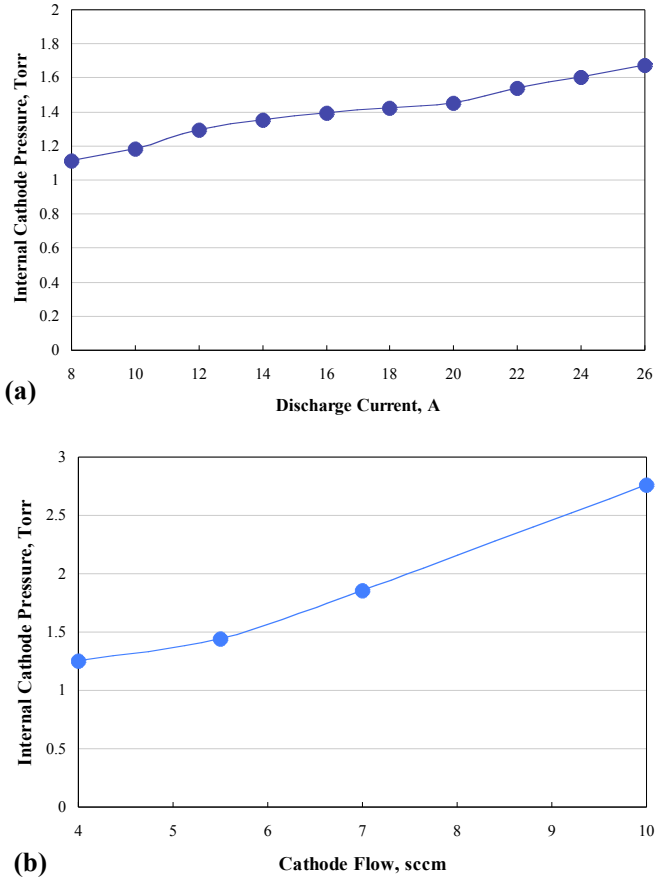

Figure 7. Internal NEXIS cathode pressure (a) constant flow rate at 5.5 sccm (b) constant discharge current at 22 A.

A. Density Measurements

The plasma density in the cathode and keeper regions is found from taking position scans with the Langmuir probe biased to ion saturation current. In this region, the plasma density is sufficiently high that the sheath is small compared to the probe radius and the probe data can be analyzed in the "thin-sheath" regime. The plasma density in the thin sheath regime is evaluated from the current[15,16] given by:

$$I = \square\, n e \sqrt{\frac{kT_e}{M}}\, A \qquad (1)$$

where $\square$ is a coefficient that changes with the geometry and the collisionality of the plasma, n is the density, e is electron charge, k is Boltzman's constant, T_e is the electron temperature, M is the ion mass, and A is the collection area of the probe. If the plasma is in a collisionless regime, _ is conventionally given as 0.5 from the Bohm current[15,16] If the plasma is in a thin-sheath but collisional regime, $\square$ ranges from 0.38 to 0.8 depending on the collisionality.[16] Since the neutral pressure inside of the NSTAR hollow cathode is very high for the all throttle level cases as shown in Fig. 6, the value for $\square$ was found to be 0.8. The neutral pressure in the NEXIS cathode is significantly lower, and $\square \approx 0.5$ was found to apply reasonably well over the operation conditions tested. The

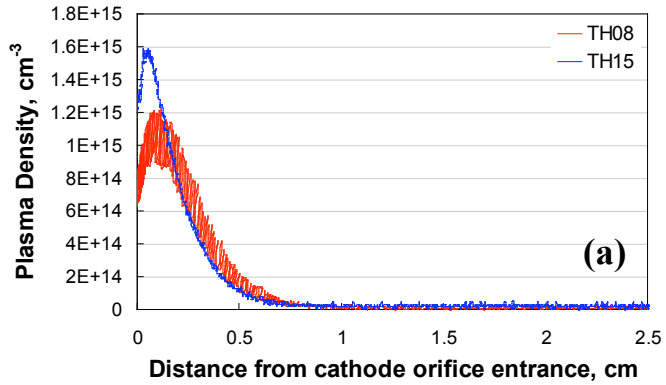

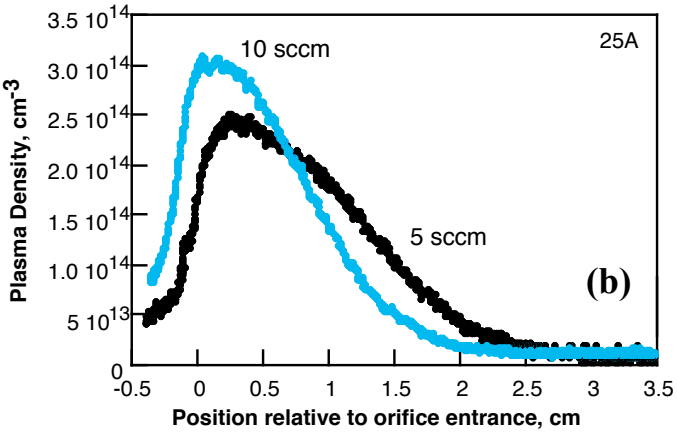

Figure 8. Cathode density profiles plotted on a linear scale for (a) the NSTAR cathode (b) the NEXIS cathode.

appropriateness of the probe theory used (thin or thick sheath) is checked periodically by calculating the ratio of the Debye length to the probe radius. The plasma enters the thick sheath regime in the anode region approximately 3 cm downstream from the keeper, where the density falls almost an order of magnitude relative to the keeper exit. When the miniature probe is found to be taking data in the thick sheath regime, a larger radius electrode is installed in the anode probe to ensure that more reliable thin sheath theory can be used. If the appropriate theory for analysis cannot be definitely determined and accurate results obtained, the data is discarded. Also, the electron temperature used for evaluating the density is obtained from the Langmuir probe data as described before.

The NSTAR throttle table is designed to keep the discharge voltage constant in the thruster while the flow rate and/or the discharge current is increased when moving from a low throttle level to a high throttle level.[14] When changing operating conditions from TH8 to TH15, which increases in both discharge current and flow rate, the density profile is shifted downstream toward the orifice and is steeper, shown in Fig. 8a. Peak plasma densities in this cathode routinely reach the low 10^{15} cm^{-3} range for TH 15, which is about 1.5 times larger than the TH8 peak density. The neutral pressure inside the cathode for TH15 is 1.6-1.7 that of TH8 which has an affect on the profiles. Higher neutral pressures in the insert region are observed to cause the cathode plasma density to decrease more rapidly upstream from the orifice. The peak plasma location is shifted downstream toward the orifice for TH15. This effect can also be seen in Fig. 8b, for the NEXIS cathode. The neutral pressure for the 10 sccm case is 1.7-1.9 times that of the 5.5 sccm case, which also causes the peak density to be pushed father downstream closer to the cathode orifice. The plasma contact area with the insert thereby decreases, suggesting that cathodes operated at pressures in the few Torr range may only utilize a fraction of the insert length for significant electron emission.[12] Surprisingly the signal for the TH8 case is much nosier than that for the TH15 case. This was also true when the probe was used to measure the floating potential. In the anode region, neither the floating potential or the ion saturation current signal were significantly more noisy for TH8 compared to TH15. It appears that the plasma in the cathode and keeper orifice regions for TH08 is inherently less stable than for TH15, probably due to the combination of gas flow and discharge current selected for this mode. The NEXIS cathode did not show any instability in the probe signal for either operation condition, suggesting that the cathode design is sufficient for the higher flow rates nominal discharge current of 25 A for this cathode.

The plasma density profiles measured inside the cathode are not only affected by the discharge current and cathode flow rate, they are also affected by the orifice size. Two different NEXIS cathode geometries were manufactured and tested. Shown in Fig. 9 are the density profiles internal to the NEXIS cathode for two different orifice sizes at 5.5 sccm and 10 sccm. Both NEXIS cathodes show that the higher flow rates cause the density peak to be pushed downstream closer to the orifice. For the 5.5 sccm case the peak density for the 2 mm orifice is about 2-3 mm downstream of the peak density for the 2.8 mm orifice case. In the smaller orifice NEXIS cathode, the orifice occupies about 13% of the diameter the cathode tube where the larger orifice occupies 19% of the cathode tube, compared to the NSTAR cathode where the orifice occupies 15% of the cathode tube. The smaller orifice size

causes a higher pressure in the cathode and orifice regions, and causes the orifice plate to run at a hotter temperature.[17]

The plasma density profiles measured by the cathode and anode probes are shown in Fig. 10a and 10b for both the NSTAR cathode and NEXIS cathode, respectively. The data for the anode region shows that the density for TH15 is 2 times larger than the density for TH8, and the plasma density in both cases falls two orders of magnitude a distance of 1-cm downstream of the keeper. Inside the cathode the density varies by 3 orders of magnitude as the probe moves upstream of the cathode orifice a distance of about 1 cm. Beyond 1 cm upstream of the cathode orifice, there is very little plasma and the current collected by the probe is in the bit noise of the data acquisition system. We expect the density to fall exponentially in this region in the manor shown by the two solid lines extending from the density curves in the cathode region. Future plans are to obtain density profiles in the cathode for the full insert length. The anode-region data taken with segmented conical anode was found to be comparable to the solid-anode NSTAR simulator geometry for both cathodes. The cathode density profiles are very different for the two cathodes. The NEXIS cathode has significant plasma density (>10^{13} cm^{-3}) nearly 3 cm upstream of the orifice at the entrance of the insert. The NSTAR cathode density decreases three orders of magnitude in 1 cm, and the plasma contact length for significant electron emission is only 2-3 mm. Tin comparison, the NEXIS cathode utilizes at least half the length of the insert for significant electron emission. The density inside of the NEXIS cathode for 25 A at 5.5 sccm is observed to be almost order of magnitude lower than the density for TH15 in NSTAR. This is consistent with a larger contact area requiring an order of magnitude lower emission current density, which reduces the required insert temperature for thermionic emission. These features were designed into the NEXIS cathode to provide extended emitter life against barium depletion.

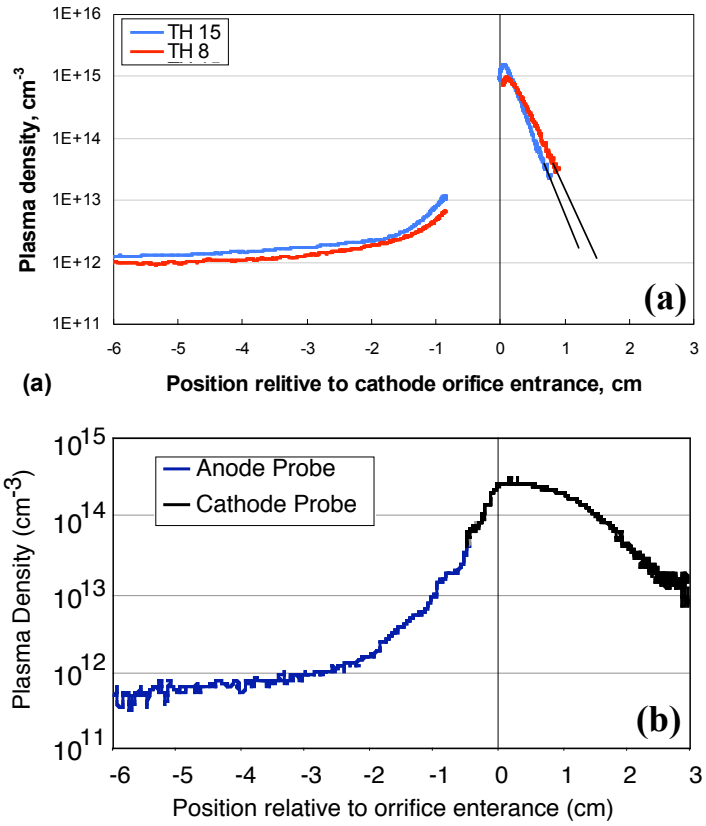

Figure 10. Axial density cathode and anode profiles plotted on a semi-log scale (a) for the NSTAR cathode (b) for the NEXIS cathode.

B. Plasma Potential and Electron Temperature Measurements

The axial plasma potential and temperature profiles for the cathodes are shown in Fig. 11, with NSTAR given in Fig.11a and NEXIS given in Fig. 11b. In Fig. 11a, the plasma potential inside the hollow cathode on axis for TH15 is found increase slightly from 4.5 V at 1 cm upstream to about 6.5 V at 0.1 cm upstream of the orifice. In the orifice the potential increases, but the perturbations to the discharge by the probe made investigating this area difficult. At TH8, the plasma potential is significantly higher than in TH15, with the potential reaching 10 V at the orifice entrance. The plasma potential in the orifice region should also increase for the TH8 case, but inserting the probe into the orifice significantly perturbed the already unstable discharge at this mode and a reliable potential measurement in the orifice could not be made. The increase in plasma potential inside the insert region at the lower TH08 discharge current clearly shows that the cathode adjusts the internal potential drop to provide adequate self-heating. At lower discharge currents, higher potential drops are needed to produce the required cathode temperature to supply the electron emission needed to support the discharge current set by the current controlled power supply. Figure 11b shows the potentials for the nominal discharge

current for the NEXIS cathode. At 25 A, the potential on axis is relatively constant at about 13 V and at the orifice the potential jumps to about 16 V. As mentioned previously the probe geometry for the NEXIS cathode allowed measurements in the orifice and into the keeper, which Fig. 11b shows that the potential continues to increase to nearly 20 V at the keeper orifice. The effect of higher flow rates at the same discharge current, shows that the potential drops about 3 V on axis and decreases less upstream where the insert is not used as efficiently, but the potential profile for 25 A at 10 sccm follows the same trend by increasing in potential in the keeper orifice to about 17 V. Increasing the gas flow rate at a fixed discharge current always decreases the discharge voltage and the

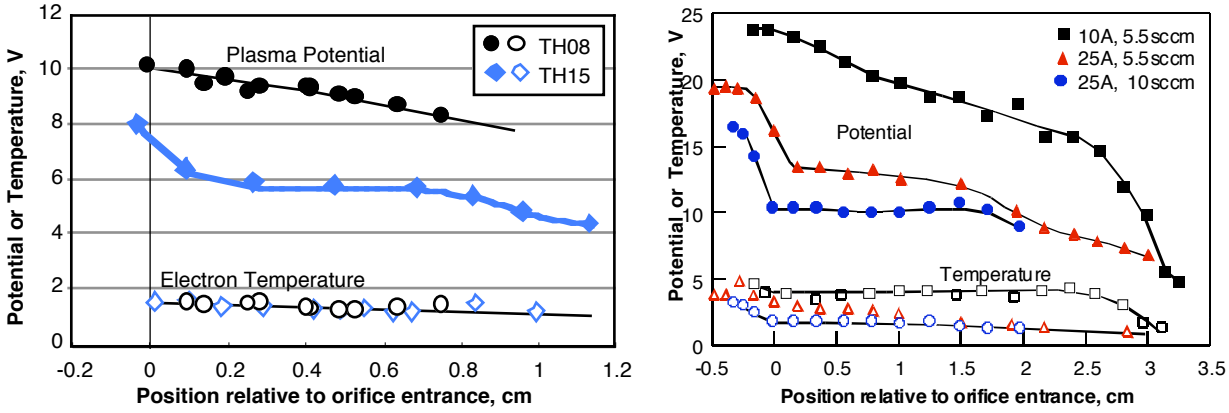

Figure 11. Plasma potential and temperature profiles for (a) for the NSTAR cathode and (b) for the NEXIS cathode.

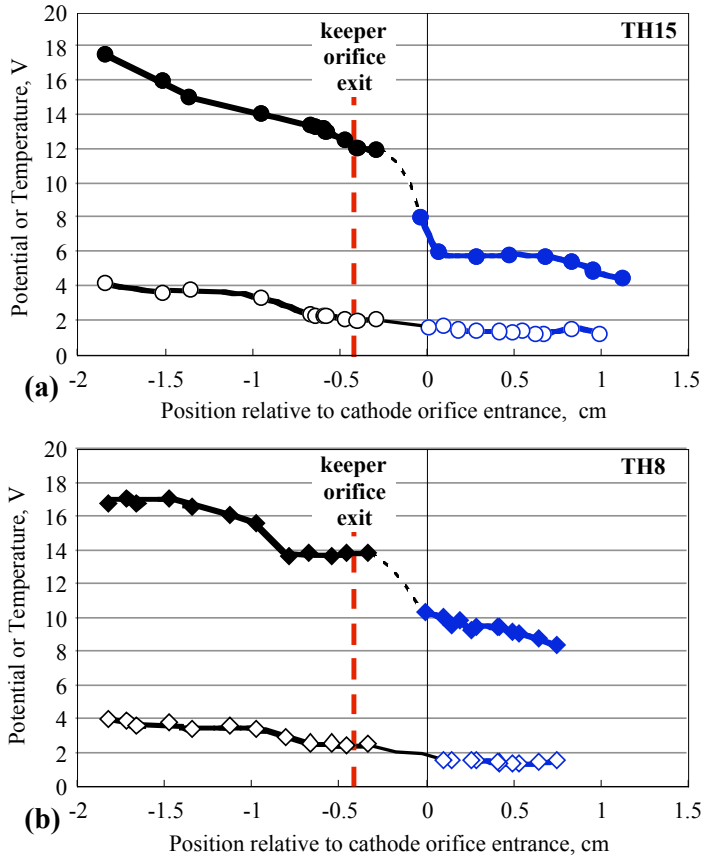

Figure 12. Plasma potential and electron temperature for the cathode-keeper region for TH15 in (a) and TH8 in (b).

electron temperature measured throughout the system. Figure 11b also shows that the NEXIS cathode is self-heating, in which at lower discharge currents the potential increases to 20-25 V in the insert region.

The potential and temperature distributions for the anode region near the keeper for TH15 and TH8 are shown in Fig. 12, along with the corresponding plasma profiles inside the cathode. The anode probe can be inserted inside the NSTAR keeper orifice, but attempts to push it deep into this region to probe the near-cathode-orifice plasma sometimes results in the probe tip striking the cathode orifice plate. Therefore, there is a discontinuity in the data in this region, indicated by the dashed lines in the figure, to avoid probe damage. Like the cathode profiles, the anode plasma potentials are dependent on the throttle level, while the electron temperatures are similar and only weekly dependent on throttle level for both throttle levels. The potential profile for TH15 shows a clear discontinuity in the cathode orifice region, where the potential increases from about 6.5 V at the cathode orifice entrance to 12 V just inside of the keeper orifice. The potential for TH8 also shows a discontinuity in this region of

approximately 4 V from the cathode orifice to the keeper orifice. The TH15 potential profile is flat for about 2 mm inside keeper orifice, and continues to increase downstream of the keeper for several centimeters. In comparison, the TH8 potential is constant over about 5 mm through the keeper orifice and then there is another 2-V potential discontinuity slightly downstream of the keeper. This downstream potential change is likely due to the discharge conditions at TH8 where the flow rate is low, the plasma density is low, and the plasma does not have enough energy to produce sufficient plasma to conduct the current to the anode. The second discontinuity is established in the potential profile to generate more plasma by accelerating the electrons to provide sufficient ionization to carry the discharge current. The plasma potential then continues to increase downstream of this region. Measurements downstream of 2 cm have been found by both Herman[7,8] and Sengupta[9] with these potential and electron temperatures for this region agree with both experiments.

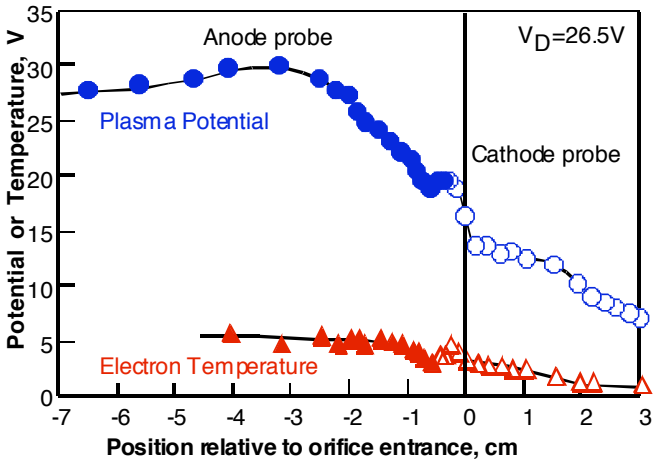

Figure 13. Plasma potential and temperature profiles for the 25 A, 5.5 sccm case.

The plasma potential and temperature profiles for the nominal NEXIS operation condition are shown in Fig. 13. In this experiment, the segmented conical anode was used and the discharge ran at 26.5 V, 25 A for 5.5 sccm of cathode flow. The plasma potential inside the hollow cathode on axis is found to be about 13 eV. The anode probe for this scan measured a plasma potential of about 19 V, which is within the accuracy of the plasma potential measurement for this region, the difference is in the error bars for the probe. For the NEXIS cathode, there is also a potential discontinuity in the cathode orifice to the keeper orifice although the probe allows measurements in this region. The potential discontinuity in the cathode orifice is normally in the 5 to 10 V range, and the plasma potential in between the orifice and keeper region is also found not to be the highest in the system. The potential is flat through the keeper orifice, and then increases downstream over several centimeters. The potential distribution observed in the cathode slowly increases to a maximum of about 30 V several cm downstream of the keeper. This is due to both the structure of the cathode plume and the increasing electron temperature observed as the probe moves downstream. The peak potential is about 3.2 V higher than the anode potential, and the plasma potential then falls downstream of the peak as the plasma density decreases further. Electron temperatures on the order of 2 to 3 eV are found inside the cathode insert and 3 to 6 eV are measured in the anode region.

The potential distribution in the anode region also changes with flow rate. Figure 14 shows the complete plasma potential and electron temperature profiles for the 25 A, 10 sccm case. Higher flow rates at a given current tend to push the first observed potential discontinuity further downstream in the cathode orifice. It is likely that smaller orifice diameters will also push the potential discontinuity down stream at the same flow rate due to the higher neutral density in the insert and orifice region. However, another potential discontinuity is observed downstream about 1 cm from the keeper exit. This profile looks similar to the NSTAR TH8 case, however the mechanism that produces the second potential discontinuity is different.

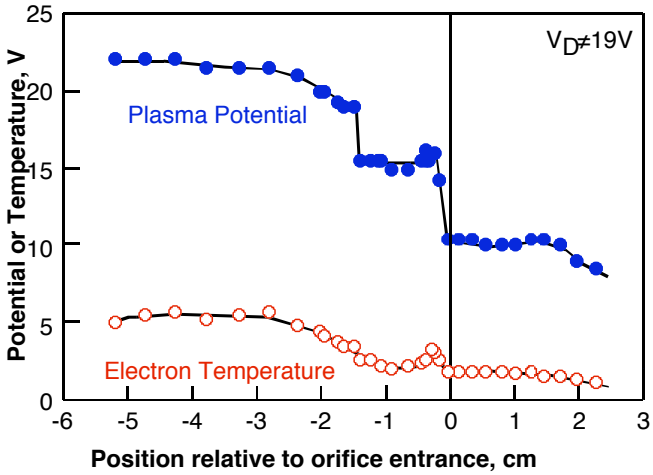

Figure 14. Plasma potential and electron temperature profiles from the 25A, 10 sccm case.

Figure 15 shows the visible emission or plasma ball from the NSTAR cathode for TH4

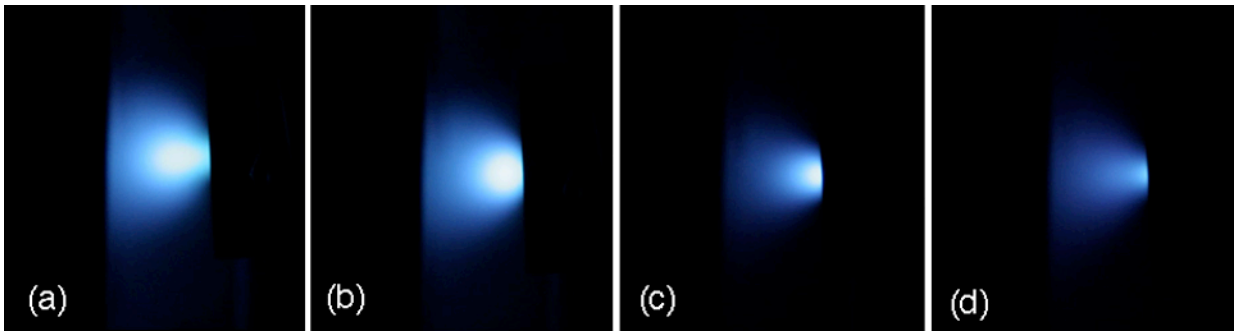

Figure 15. Plasma ball in the NSTAR cathode plume for TH15 (a), TH12 (b), TH8 (c), and TH4 (d).

TH8, TH12, and TH15; while Fig. 16 shows the plasma ball for the NEXIS cathode at 25 A for 5.5 and 10 sccm. Exterior to the keeper, the axial extent of the plasma ball changes dramatically with flow and discharge current, and this effect can be seen in both Figs. 15 and 16. Higher flows tend to move the ball downstream, often exposing a classic Faraday dark space between the ball and the plasma located between the keeper and the cathode orifices. Higher currents tend to enlarge the ball and increase the plasma density, as does the application of an axial magnetic field, due to enhanced ionization. In NSTAR, the plasma ball extends from the keeper orifice out a few millimeters downstream into the anode plasma. From Fig. 15, as the pictures progress to lower throttle levels it can be seen that the plasma-ball is pulled into the keeper. During TH8 operation, the ball is pulled partially inside the keeper and just the tail end of the ball can be seen at the downstream end of the keeper orifice, as shown in Fig. 13(c). This suggests there is week ionization just downstream of the keeper, leading to the potential profile seen in Fig. 12b. However the potential profile observed for the NEXIS cathode at 10 sccm, can be explained by the optical emission photograph shown Fig. 16b. The plasma ball is moved significantly downstream of the keeper orifice and at this high flow rate a dark space is clearly observed. The dark space corresponds to a region of low electron temperature where excitation is decreased. However, this reduced-luminosity region also is observed in the 5.5 sccm case, although it is closer to the keeper and less apparent in the photograph. The constant potential the keeper orifice for the 10 sccm case to 1 cm downstream can also be explained by the plasma not having sufficient energy to produce plasma conduct the discharge to the anode due to the dark space observed in the photograph.

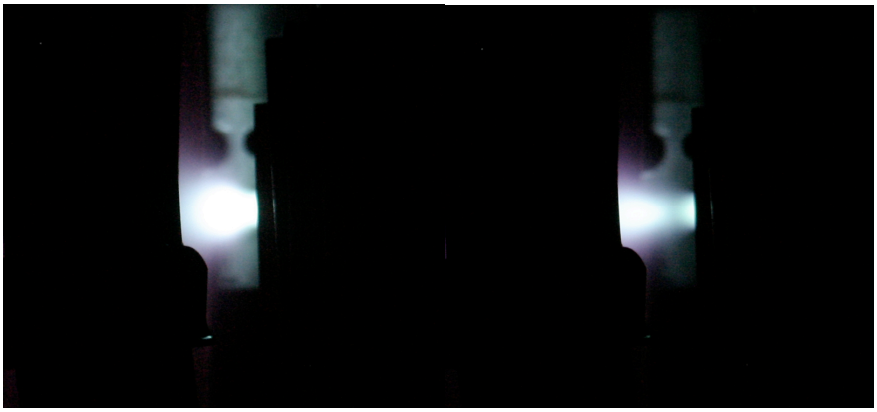
Figure 16. Plasma ball in the NEXIS cathode plume for 25 A discharge for (a) 5.5 sccm and (b) 10 sccm.

IV. Discussion of the Plasma Profiles

Investigation of the hollow cathode plasma and plume shows that the plasma parameters and profiles are significantly affected by cathode and anode geometries, as well as operating conditions. The motion and shape of the visible plasma ball present in both the NSTAR and NEXIS cathode plumes suggests that this area in the discharge chamber plays a significant role in conducting the discharge current to the anode. To provide some electrical measurements to relate to the visual differences observed in the plasma plume as the operation parameters are changed, the segmented conical anode shown in Fig. 4a was installed to measure the current distribution along a conical-anode wall near the cathode plume. For the NEXIS cathode at the nominal operating point, the current to each of the six independently monitored anode segments is shown in Fig. 17. We see in Fig. 17a that without an applied axial magnetic field at the cathode, a large fraction of the discharge current goes to the first ring and the current to each successive ring decreases monotonically. This is consistent with the rapidly decreasing plasma

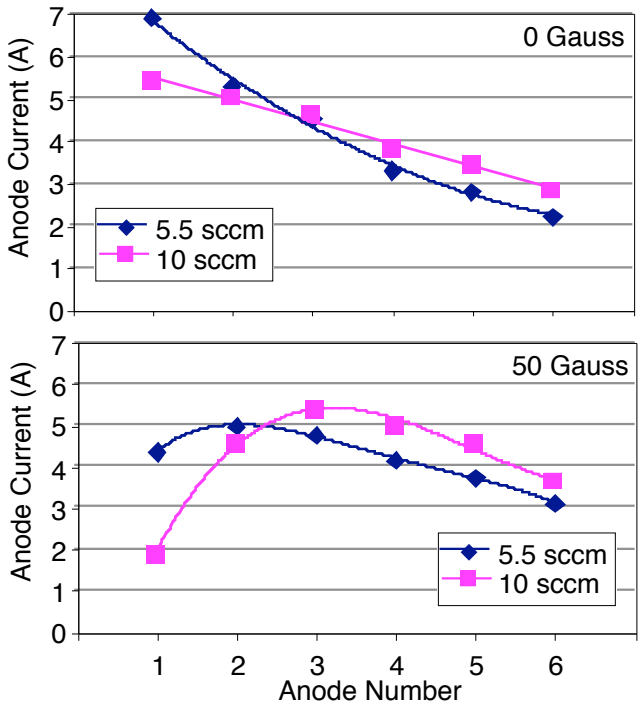

Figure 17. Anode currents to the segmented anode for the nominal NEXIS case of 25 A and 5.5 sccm.

density profile shown in Fig. 10 and the increasing collection area of each successive ring as you move away from the cathode exit. However, when the cathode flow is increased to 10 sccm at the same 25 A discharge current, the current collected by the first ring decreases and the downstream anode-rings collect correspondingly more electrons. This is consistent with the plasma ball pushing downstream into the discharge chamber at higher flows, which increases the plasma density downstream and provides more current to the downstream segments. A similar effect is seen in Fig. 17b when an axial magnetic field is applied using the solenoid coil positioned around the cathode. The current collected by the first anode-ring decreases by over 60% with this field, and the peak current collection is shifted downstream. The applied magnetic field has two effects: first the plasma ball moves downstream in the same manner as increasing the flow, as seen visually in Fig. 16, and second, the magnetic field provides some plasma confinement that reduces the radial electron flux to the anode segments near the cathode where the plasma is magnetized. If the gas flow is then increased to 10 sccm at the same discharge current, as shown in Fig. 17b, the reduction in the currents collected by the first ring becomes even more significant, and the plasma pushes even farther downstream.

The discharge stability depends on the discharge parameters and the anode configuration. Figure 18 shows the discharge voltage and current for the NEXIS cathode operating at 5.5 sccm with the cylindrical anode shown in Fig. 4a and the segmented anode shown in Fig. 4b. The cylindrical anode runs stably from less than 10 A to over 50 A, while the segmented cylindrical anode has regions between 10 and 16 A and above 26 A where the discharge is unstable. In the 10 to 16 A region with the segmented anode, the discharge exhibited the sudden onset of large amplitude, high frequency voltage oscillations. Above 25 A, the discharge oscillations tended to increase in amplitude with increasing discharge current. Increasing the gas flow or applying an axial magnetic field from the cathode solenoid tended to damp these oscillations and increase the range over which the discharge could run stably with the conical anode.

In addition to the general stability exhibited by the cylindrical anode, the discharge voltage shown in Fig. 18 was significantly reduced compared to the conical anode. This is due to the confinement of the gas in the plasma plume region, which lowered the discharge voltage and made the plasma more stable by increasing the plasma generation rate in this region. This same affect could be achieved with the conical anode by the injection of additional gas into the vacuum system from a separate gas feed. This is reminiscent of increasing the main flow rate into the discharge chamber in ion thrusters, which normally reduces the discharge voltage. However, the main chamber flow rate in our experiments had to be over twice the cathode flow rate to cause the discharge voltage in the conical anode configuration to approach the voltage in the cylindrical anode configuration. This is clearly due to the fact that the ability of the discharge to conduct current to the anode is related to the plasma density in the cathode plume region,

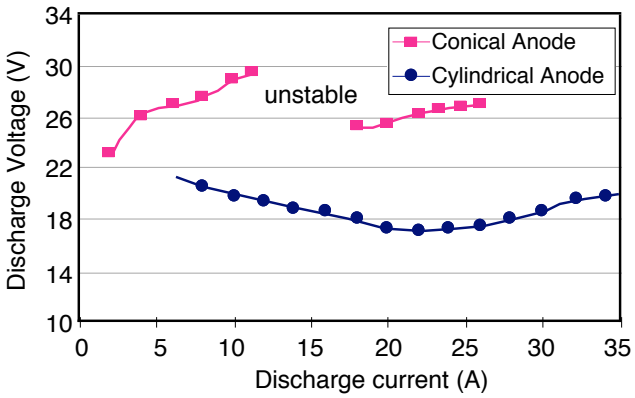

Figure 18. Discharge current and voltage with the NEXIS cathode for two anode configurations.

the ionization rate of which is enhanced by efficient confinement of the gas flow from the cathode with the small cylindrical anode. Since the discharge voltage and stability is related to the anode geometry, any extended testing of hollow cathodes should be configured with realistic anode and magnetic field geometries to provide an environment for the cathode that is representative of the final application. This will ensure that the potential profiles and ion energies that determine the sputter-erosion and life of the cathode are replicated in the life test.[18]

The radial scanning probe was used to investigate the potential structure of the cathode plume and the plasma ball under the discharge conditions examined here. For the NSTAR cathode, the plasma-ball in TH15 is clearly visible in Fig. 15a, and has a diameter of about 1 cm. The radial profile of the time-average plasma potential measured 2 mm in front of the keeper for TH15 is shown in Fig. 18. The potential is clearly depressed to about 12 V on axis directly in the cathode plume, and increases as the probe moves out radially. The potential increases rapidly as the probe encounters the edge of the plasma ball, at about 0.5 cm from the axis. From that point the potential increases to a value above the discharge voltage, which extends out to near the anode electrode. The NEXIS cathode plume at 25 A for 5.5 sccm, seen in Fig. 16a, has a plasma ball structure similar to that of the NSTAR cathode at TH15, but the ball is located somewhat farther out from the keeper. The radial potential profiles are shown in Fig. 19 for the NEXIS cathode plume and the conical-cylindrical anode configuration shown in Fig. 4c. This is similar in shape to the profile for the NSTAR cathode, except that potential change is more gradual and continues to increase to over 35 V as the probe moves closer to the anode. As the probe is positioned further downstream from the keeper, the plasma potential begins flatten out as the plume disperses and the plasma becomes more uniform. This dispersion of the cathode plume is illustrated in Fig. 20, where the density profiles for the NEXIS cathode for the nominal operating condition are shown. The plasma density is peaked on axis, and density decreases in magnitude radially corresponding to the dispersion of plasma. Figure 20 also shows that the density falls about an order of magnitude axially over 2 cm, corresponding well to the axial data scan shown in Fig. 10b.

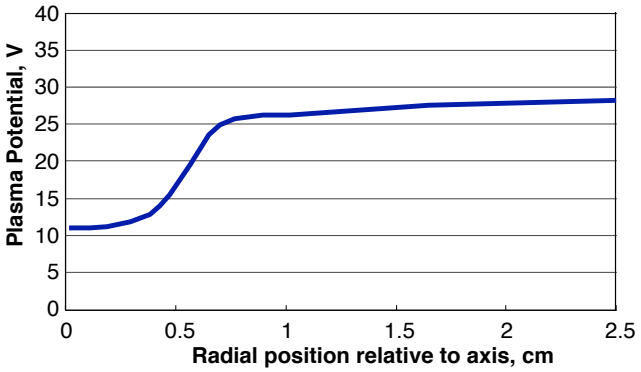

Figure 18. Time averaged radial profile of plasma potential for TH15 from an emissive probe.

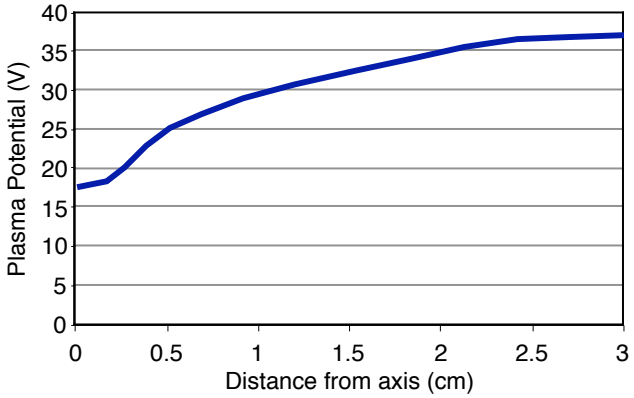

Figure 19. Time averaged radial profile of plasma potential for the NEXIS cathode for 25 A at 5.5 sccm.

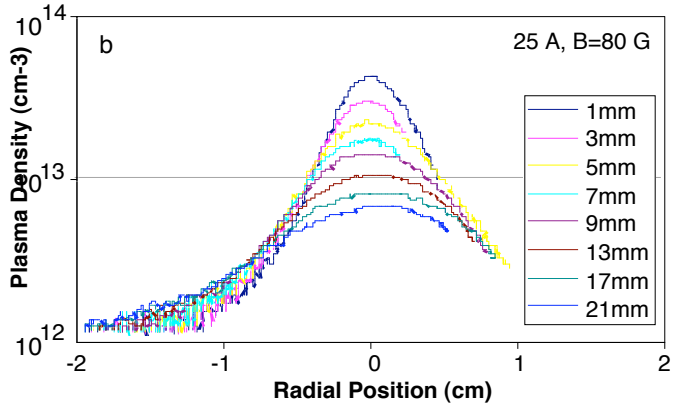

Figure 20. Plasma density radial profile for the NEXIS cathode for 25 A at 5.5 sccm.

Since the shape of the anode electrode can strongly affect the discharge voltage, the potential and temperature profiles in the cylindrical anode case for the NEXIS cathode operating at 25 A and 5.5 sccm were examined and are shown in Fig. 21. The plasma potential in the cathode insert and orifice regions is essentially unchanged for the cases previously shown with the conical anodes. Modification of the anode geometry does not affect the basic cathode operation because these potentials and

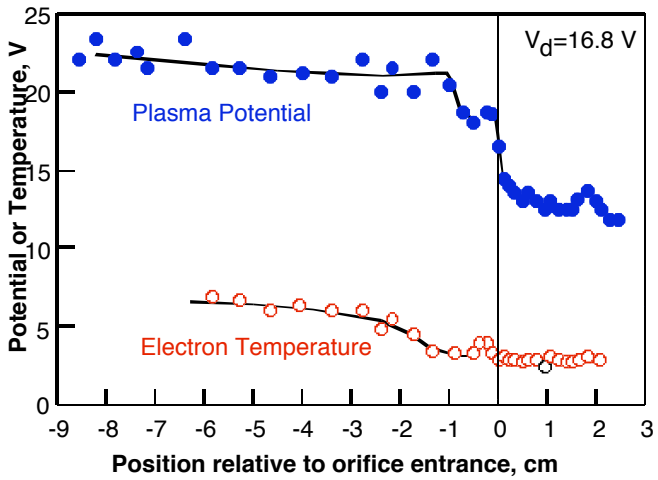

Figure 21. Plasma potential and electron temperature for the nominal 25A case with the cylindrical anode.

temperatures are sufficient to deliver the desired discharge current at the given cathode flow rate. The anode geometry changes the potential structure exterior to the cathode in the anode-plasma region at a given current and gas flow. As seen in Fig. 21, the potential increases to about 5 V positive relative to the anode potential and is then relatively flat over the axial probe scanning distance. The conical anode also showed plasma potentials 3 to 4 V above the anode voltage, but the discharge required higher total voltages to generate the anode plasma and conduct the current the anode. This is likely because the gas density is significantly lower in the anode region in the conical anode case. This implies that larger thrusters with anodes farther away from the cathode may require higher cathode flow rates to operate at the same discharge voltage as smaller thrusters.

Finally, both hollow cathodes showed clear indications of short-term and long-term conditioning. When first turning on a hollow cathode with a new insert, the discharge voltage is observed to decrease several volts gradually over some ten's of hours, and then increase very slowly on the order of 1 to 2 V over several hundred hours before stabilizing. If exposed to air for any significant time, the discharge voltage at a given current and flow rate would increase 2 to 3 V, and then require on the order of 10 hours to fully recover. The probe data showed that the plasma potential inside the insert region tracked the discharge voltage closely. Environmental effects that might affect the insert work function are handled in the self-heated cathode by the plasma increasing the power delivered to the cathode insert, which increases the insert temperature sufficiently to provide the required electron emission. The power deposition is increased by the higher plasma potential in the insert region, which appears as a larger voltage drop in the hollow cathode plasma. Since the discharge voltage is the sum of the hollow cathode voltage drop and the voltage drop in the anode plasma exterior to the cathode, changes to the internal sheath potential required to heat the cathode insert show up as changes in the discharge voltage. This conditioning and history dependence of the hollow cathode will be further studied in the future to determine its impact on the life and reliability of these cathodes in ion thrusters.

V. Conclusion

Probe studies of hollow cathode discharges have provided considerable insight into the plasma structure upstream and downstream of the cathode orifice; specifically the potential, density, temperature profiles throughout the system. The use of miniature, high-speed scanning probes permitted high-density regions to be investigated and mapped where the plasma was too intense for slow or stationary probes to be used. This work has demonstrated that the potential structure in hollow cathode discharges varies significantly with discharge current, flow rate, anode geometry and cathode geometry. The plasma parameters and profiles presented here are crucial for benchmarking cathode and plasma discharge chamber models used to predict ion thruster performance and life. Since the data presented is only for two operating conditions for both the NSTAR and NEXIS hollow cathode geometries, future work will expand on the operating conditions, geometry and time dependence of the cathode performance to aid in constructing comprehensive models of the hollow cathode discharge.

Acknowledgments

The research described in this paper was carried out by the Jet Propulsion Laboratory, California Institute of Technology, under a contract with the National Aeronautics and Space Administration in support of Project Prometheus.

References

[1]A. Sengupta, J. Brophy, K. Goodfellow, "Status of the Extended Lift Test of the Deep Space 1 Flight Spare Ion Engine After 30'352 Hours of Operation", AIAA Paper #2003-4558, 39th Joint Propulsion Conference, Huntsville, AL, July 20-23, 2003.

[2]Lidsky, L., Rothleder, J. Rose, D., Yoshikawa, S., Michelson, C., Mackin, J. Appl. Phys. **22** (1962) p.2490.

[3]Rawlin, V., Pawlik, E., "A Mercury Plasma Bridge Neutralizer", *J. Spacecraft Rockets*, **5** (1968) p.814.

[4]Moore, R. "Magneto-Electrostatically Contained Plasma Ion Thruster", AIAA Paper #69-260, 7th Electric Propulsion Conference, Williamsburg, VA, March 3-5, 1969.

[5]Sovey, J. "Performance of a Magnetic Multipole Line-Cusp Argon Ion Thruster", AIAA Paper #81-0745, AIAA Electric Propulsion Conference, Las Vegas, Nevada, April 21-23, 1981.

[6]Siegfried, D. and Wilbur, P., "An Investigation of Mercury Hollow Cathode Phenomena", AIAA Paper #78-705, 13th International Electric Propulsion Conference, San Diego, CA, April 25-27, 1978.

[7]Hayakawa, Y., Miyazaki, K., Kitmuira, S., "Measurements of Electron Energy Distributions in a 14 cm Diameter Ring-Cusp Ion Thruster", AIAA Paper #89-2715, 25th Joint Propulsion Conference, Monterey, CA July 10-12, 1989.

[8]D.Herman and A.Gallimore, "Discharge Chamber Plasma Structure of a 30-cm NSTAR Ion Engine", AIAA Paper #2004-3794, 40th Joint Propulsion Conference, Ft. Lauderdale, FL, July 11-14, 2004.

[9]D.Herman and A.Gallimore, "Comparison of Discharge Plasma Parameters in a 30-cmNSTAR Type Ion Engine with and without Beam Extraction", AIAA Paper #2003-5162, 39th Joint Propulsion Conference, Huntsville, AL, July 20-23, 2003.

[10]A.Sengupta, D.M. Goebel, D. Fitzgerald, A. Owens, "Experimentally Determined Neutral Density and Plasma Parameters in a30 cm Ion Engine", AIAA Paper #2004-3613, 40th Joint Propulsion Conference, Ft. Lauderdale, FL, July 11-14, 2004.

[11]D.Herman and A.Gallimore, "Near Discharge Cathode Assembly Plasma Potential Measurments in a 30-cm NSTAR-type Ion Engine amist Beam Extraction", AIAA Paper #2004-3958, 40th Joint Propulsion Conference, Ft. Lauderdale, FL, July 11-14, 2004.

[12]D.M.Goebel, K.Jameson, R.Watkins, I.Katz, "Hollow Cathode and Keeper-Region Plasma Measurements Using Ultra-Fast Miniature Scanning Probes", AIAA Paper #2004-3430, 40th Joint Propulsion Conference, Ft. Lauderdale, FL, July 11-14, 2004.

[13].K. Jameson, D.M. Goebel, R. Watkins, "Hollow Cathode and Keeper-Region Plasma Measurements", AIAA Paper #2005-3667, 41th Joint Propulsion Conference, Tuscan, AZ, July 10-13, 2005.

[14]J. Brophy, "NASA's Deep Space 1 Ion Engine", Rev. Sci.Instrum. **73** (2002) p.1071-1078

[15]F.Chen, ""Electric Probes", in *Plasma Diagnostics Techniques* (ed. R. Huddelstone and S. Leonard), Academic Press, NY (1966) p. 113-200.

[16]D.Bohm, *The Characteristics of Electrical Discharges in Magnetic Fields*, edited by A. Gutirie and R.K. Wakerling (McGraw-Hill, New York, 1949) Chap.3.

[17]I. Katz, et al., "Combined Plasma and Thermal Hollow Cathode Insert Model" IEPC 2005-228, International Electric Propulsion Conference, Princeton, NJ, Oct.31st-Nov.4th, 2005.

[18]D.M.Goebel, K.Jameson, R.Watkins, I.Katz, et al., "Energetic Ion Production and Keeper Erosion in Hollow Cathode Discharges" IEPC 2005-266, International Electric Propulsion Conference, Princeton, NJ, Oct.31st-Nov.4th, 2005.